

1 **Carbon Exchange between the Atmosphere and Subtropical**
2 **Forested Cypress and Pine Wetlands**

3

4 **W. Barclay Shoemaker¹, Frank Anderson², Jordan G. Barr³, Scott L. Graham⁴, and**
5 **Daniel B. Botkin⁵**

6

7 [1] U.S. Geological Survey, Florida Water Science Center, 7500 SW 36th St, Davie, FL 33314,
8 bshoemak@usgs.gov, 954-377-5956

9 [2] U.S. Geological Survey, California Water Science Center, Placer Hall, 6000 J Street, Sacramento, CA,
10 fanders@usgs.gov, 916-2783258

11 [3] South Florida Natural Resource Center, Everglades National Park, Homestead, FL 33030

12 [4] NIWA Taihoro Nukurangi, Riccarton, Christchurch, NZ

13 [5] Department of Biology, University of Miami, Coral Gables, FL, USA

14

15

16

17 **Abstract**

18 Carbon dioxide exchange between the atmosphere and forested subtropical wetlands is
19 largely unknown. Here we report a first step in characterizing this atmospheric-ecosystem
20 carbon (C) exchange, for cypress strands and pine forests in the Greater Everglades of Florida as
21 measured with eddy covariance methods at three locations (Cypress Swamp, Dwarf Cypress and
22 Pine Upland) for two years. Links between water and C cycles also are examined at these three
23 sites, and methane emission measured only at the Dwarf Cypress site. Each forested wetland
24 showed net C uptake from the atmosphere both monthly and annually, as indicated by net
25 ecosystem exchange (NEE) of carbon dioxide (CO₂). For this study, NEE is the difference
26 between photosynthesis and respiration, with negative values representing uptake from the
27 atmosphere that is retained in the ecosystem or transported laterally via overland flow
28 (unmeasured for this study). NEE was greatest at the Cypress Swamp (-900 to -1000 g C per m²
29 year), moderate at the Pine Upland (-650 to -700 g C per m² year), and least at the Dwarf
30 Cypress (-400 to -450 g C per m² year). Changes in NEE were clearly a function of seasonality
31 in solar insolation, air temperature and flooding which suppressed heterotrophic soil respiration.
32 We also note that changes in the satellite-derived enhanced-vegetation index (EVI) served as a
33 useful surrogate for changes in -NEE at these forested wetland sites.

34

35 **1 Introduction**

36 At global scales, wetlands are generally considered sinks for atmospheric carbon dioxide
37 (Troxler et al. 2013, Bridgham et al., 2006) and natural sources for methane emission (Whalen
38 2005, Sjogersten et al. 2014). Wetlands in southern Florida's greater Everglades
39 (<http://sofia.usgs.gov/>) are expansive subtropical ecosystems that are carbon (C) accumulating
40 over geologic time scales (Jones et al., 2014). Here we report a first step in characterizing
41 modern rates of atmospheric-ecosystem carbon (C) exchange, for cypress strands and pine
42 forests in the Greater Everglades of Florida.

43 In addition to the insight provided on the role of subtropical forested wetlands in the
44 global carbon cycle, this research is expected to be useful for determining consequences of land-
45 use changes in the Everglades region. Canal building and drainage projects in south Florida have
46 reduced the original extent of the Everglades (Parker et al., 1955), decreased peat accretion rates
47 and total carbon stocks, and reduced ecosystem services. Hohner and Dreschel (2015), for
48 example, estimate the Greater Everglades has less than 24% its original peat volume and 19% of
49 its original carbon. In response, State and Federal governments are planning and executing
50 complex projects to restore Everglade's wetlands (<http://www.evergladesplan.org/>) while
51 concurrently avoiding flooding in urbanized areas and maintaining water supply.

52 Restoring ecosystems will affect water, energy and C cycles, as plants and soil processes
53 adjust to changing water levels, salinities, nutrient loads and fire regimes. For example, Jimenez
54 et al. (2012) and Schedlbauer et al. (2010) indicate that additional deliveries of water into peat
55 and marl saw grass wetlands may diminish C accumulation within these wetlands. Eddy-
56 covariance derived estimates of net ecosystem productivity declined with increasing inundation

57 during the wet season (Jimenez et al., 2012; Schedlbauer et al., 2010). These results were
58 partially attributed to the amount of vegetation that, due to flooding, could not directly exchange
59 carbon dioxide with the atmosphere. The opposite trend was observed in a tidally influenced
60 mangrove forest in Everglades National Park. Lowered salinities, resulting from increased
61 freshwater flow, resulted in increased daily PAR-use efficiency (i.e. ratio of gross ecosystem
62 productivity to photosynthetically active irradiance (PAR), (Barr et al., 2010; Barr et al., 2012).
63 Also, ecosystem respiration losses were lower during periods of inundation (Barr et al., 2010;
64 Barr et al., 2012), which increased net C uptake over the mangrove forest. These studies provide
65 insights on water and C cycling over coastal sawgrass wetlands and mangrove forests. C cycling
66 over other subtropical wetlands, such as cypress strands and pine forests, is largely unstudied
67 (Sjogersten et al. 2014).

68 The primary goal of this paper is to quantify the magnitude and controls of C exchange
69 within cypress and pine forested wetlands. These wetland communities are defined by
70 McPherson (1973) and Duever et al. (1986, 2002). Quantities of interest include net
71 atmospheric/ecosystem C exchange (NEE), ecosystem respiration (RE), gross ecosystem
72 exchange (GEE), and methane emissions. Latent heat flux (LE) and evapotranspiration (ET)
73 also are quantified so that links between water and C cycles can be quantitatively studied. We
74 address several specific objectives on daily, monthly and annual time scales, including (1) the
75 magnitude of cypress (tall and dwarf) and pine forested wetlands as net atmospheric C sources or
76 sinks, (2) site differences in water and C exchange metrics (i.e., -NEE, GEE, RE, and surface
77 energy fluxes), and (3) the magnitude of methane emission over a dwarf cypress wetland.
78 Results from this study are expected to help define and predict responses of subtropical forested

79 wetlands to regional (e.g., freshwater discharge) and global (e.g., air temperature) environmental
80 change.

81 **2 Methods**

82 **2.1 Site Description**

83 The study area is the Big Cypress National Preserve (BCNP) in southern Florida (Figure
84 1). A variety of subtropical forested and non-forested wetland ecosystems are present in BCNP,
85 including Pine Upland, Wet Prairie, Marsh, Hardwood Hammocks, Cypress Swamps, Dwarf
86 Cypress and Mangrove Forests as formally characterized by McPherson (1973) and Duever et al.
87 (1986, 2002). The distribution of ecosystems and plant communities in the BCNP is controlled
88 by topography, hydrology, fire regimes, and soil conditions (Duever et al., 1986). Marsh,
89 Cypress Swamp, and Mangrove Forests typically occupy low elevations (< 2.5 m National
90 Geodetic Vertical Datum, NGVD-29), Wet Prairie occupies middle elevations (3 to 4 m NGVD-
91 29), and Pine Uplands and Hardwood Hammocks occupy high elevations (>4 m NGVD-29).
92 These wetlands provide floodwater protection, hurricane buffering, substrate stabilization,
93 sediment trapping, water filtration, and other ecosystem services for urban areas and coastal
94 estuaries.

95 Water and C fluxes were determined over Pine Upland, Cypress Swamp and Dwarf
96 Cypress ecosystems (Figure 1, Table 1) from December 2012 to November 2014 (Shoemaker et
97 al., 2015d, e, f). The Pine Upland site (Figure 2, Table 1), is classified as a mixed lowland pine
98 site, and is located in an extensive open-canopy pine forest with numerous small- to medium-
99 sized cypress domes. The canopy is dominated by slash pine (*Pinus elliottii*) with an understory
100 of saw palmetto (*Serenoa repens*), small trees and shrubs including holly (*Ilex cassine*), swamp
101 bay (*Persea palustris*), myrsine (*Myrsine cubana*), and wax myrtle (*Myrica cerifera*), and

102 scattered sabal palms (*Sabal palmetto*) (Figure 2). The ground cover is a diverse mix of short
103 (less than 1 m) grasses, sedges, and forbs that are scattered in open-to-dense patches around the
104 site. The open character of the site indicates regular burning with fire recurrence every 5 years,
105 on average. Large cypress domes have a dense canopy of cypress, but open subcanopy and
106 shrub strata, probably due to frequent fires. Substrates are primarily limestone bedrock, with
107 sandy marl in the shallow depressions. Cypress domes in the area have a shallow organic
108 substrate in the deeper areas.

109 The Cypress Swamp site (Figure 2, Table 1) is classified as a swamp forest (Duever et
110 al., 1986) and supports a tall dense cypress forest with a subcanopy of mixed hardwoods (Figure
111 2). Plant varieties include bald cypress (*Taxodium distichum*), holly, swamp bay, maple (*Acer*
112 *rubrum*), an open-to-dense shrub layer with coco plum (*Chrysobalanus icaco*), myrsine, wax
113 myrtle, an open-to-dense ground cover of swamp fern (*Blechnum serrulatum*), and a variety of
114 grasses, sedges, and forbs. The substrate is primarily topographically irregular limestone
115 bedrock with organic accumulations in depressions in the rock.

116 The Dwarf Cypress site is classified as scrub cypress and is dominated by cypress,
117 *Taxodium distichum*, and scattered (5 to 10 percent cover) sawgrass less than 1 m high (Figure
118 2). Small to medium-sized cypress domes are present, and periphyton is seasonally abundant
119 (Figure 2) from about July to December. The substrate is shallow marl overlying
120 topographically irregular limestone bedrock.

121 **2.2 Carbon Balance**

122 A mass balance equation can be used to conceptualize C fluxes. Net ecosystem C
123 balance (NECB) is the amount of C accumulating in the ecosystem, in units of mass per area
124 time (Chapin et al. 2006, Troxler et al., 2013). NECB can be partly approximated using eddy-
125 covariance methods by measuring (1) the net vertical (1-dimensional) exchange of carbon

126 dioxide (-NEE) across the ecosystem-atmosphere interface, (2) the net lateral flux (F_{net}) of
127 dissolved/particulate organic/inorganic C leaving the system, and (3) the C released from
128 methane emission (F_{CH4}):

$$129 \quad NECB = -NEE - F_{net} - F_{CH4} \quad (1)$$

130 A negative sign for NEE indicates a loss of carbon dioxide from the atmosphere. The net
131 lateral flux of C (F_{net}) occurs primarily within surface water that flows down topographic
132 gradients toward mangrove wetlands on the coast (Figure 1). Technical difficulties inherent in
133 measuring “sheet flow” and the dissolved/particulate organic/inorganic C concentrations within
134 surface water did not allow quantification of this term. Therefore, we only report exchanges of
135 gases between the atmosphere and the ecosystem. Methane emission (F_{CH4}) at the Dwarf
136 Cypress site was determined using a LICOR-7700 open-path methane analyzer (Shoemaker et
137 al., 2015d). The cost of the methane analyzer and safety issues related to climbing tall towers
138 limited measurements of F_{CH4} to a single site (Dwarf Cypress, Figure 2). Thus, our daily and
139 annual NEE estimates likely are an upper bound for C accumulation at the Pine Upland and
140 Cypress Swamp sites (and lower bound for atmospheric transfer to the ecosystem) due to
141 uncertainty associated with methane emission and lateral C fluxes.

142 **2.3 Eddy Covariance Method and Gap-filling**

143 The eddy covariance method (Dyer, 1961; Tanner and Greene, 1989) is a one-
144 dimensional (vertical) approach for measuring the exchange of gases within the atmospheric
145 surface layer (Campbell and Norman, 1998). Key instrumentation (Table 2) includes sonic
146 anemometers that rapidly (10-Hz) measure wind velocity and gas analyzers that rapidly measure
147 gas concentrations (Table 2) in the atmosphere. The covariance between vertical wind velocities
148 and gas concentrations determines the net exchange of gases between the ecosystem and

149 atmosphere. Additional instrumentation (Table 2) was installed at each site to measure net
150 radiation, soil-heat flux, soil temperatures, air temperature and relative humidity, and distance of
151 water above or below land surface (using pressure transducers). Pressure transducers were
152 placed in the bottom of groundwater wells to measure the distance of water above and below
153 land surface. Pressure transducers were corrected monthly for instrumentation drift using
154 manual depth-to-water measurements from the top of the well casings. The manual depth-to-
155 water measurements allowed precise calibration of continuous water distance above or below
156 land-surface. Monthly site visits were made to download data, perform sensor inspections and
157 complete other site maintenance. All instrumentation was visually inspected, leveled, cleaned, or
158 replaced as necessary.

159 Raw, 10-Hz, vertical wind speed, temperature, and gas concentration data were processed
160 to half-hourly fluxes using EddyPro software (version 4.0.0) following advanced protocols that
161 included random uncertainty estimates (Finkelstein and Sims, 2001), spiking filters, double
162 coordinate rotations, blocked-average detrending, statistical filters, air density and oxygen
163 corrections (Tanner and Thurtell , 1969; Baldocchi et al., 1988; Webb et al., 1980; Tanner et al.
164 1993), and high-pass filtering. Processed data yielded half-hourly mean values of NEE,
165 methane, sensible and latent heat fluxes that were filtered to remove periods with unrealistic
166 fluxes (*Cypress Swamp* - latent heat fluxes >800 and <-100 watts m^{-2} , sensible heat flux >500
167 and <-150 , NEE >25 and <-30 $\mu\text{mol m}^{-2} s^{-1}$; *Dwarf Cypress* - latent heat fluxes >600 and <-150
168 watts m^{-2} , sensible heat flux >500 and <-100 , NEE >20 and <-25 $\mu\text{mol m}^{-2} s^{-1}$, FCH4 >0.5 and
169 <-0.2 ; *Pine Upland* - latent heat fluxes >1000 and <-300 watts m^{-2} , sensible heat >500 and <-200
170 watts m^{-2} , NEE >125 and <-100 $\mu\text{mol m}^{-2} s^{-1}$. These thresholds may inherently disregard some
171 naturally large uptake or efflux events. For instance, ebullition events can be an important

172 mechanism for episodic release of methane to the atmosphere (Comas and Wright, 2012).

173 However, at present, the drivers of these events are not well understood and thus difficult to
174 model with physiological-based gap-filling procedures.

175 Following EdiPro processing, local despike and friction velocity filters were applied to
176 the gas fluxes (Shoemaker et al., 2015d, e, f). The local despike filter removed half-hour fluxes
177 that fell outside 3 standard deviations of the fluxes within a moving 7-day window. Friction
178 velocity is an indicator of time periods when turbulent wind conditions are well developed.

179 Eddy covariance methods are appropriate for turbulent wind conditions. The u^* threshold was
180 selected based on plots of u^* versus nighttime (9PM to 4AM) NEE normalized by air
181 temperature and vapor pressure deficit, as described by Aubinet et al. (2012, pg. 147). NEE
182 appeared to be considerably different as u^* decreased approximately below 0.1 threshold.

183 Roughly 25, 17, and 21 percent of NEE values were removed by the u^* , local despike and
184 unrealistic value filters at the Cypress Swamp, Dwarf Cypress and Pine Upland sites,
185 respectively.

186 At the Pine Upland site, NEE contamination was possible due to fossil fuel combustion
187 by generators and trucks supporting oil-drilling activities adjacent to the eddy-covariance tower.
188 Thus, all carbon fluxes were removed at Pine Upland when the wind direction was from the east
189 of the tower (15 to 130°). This filter removed about 50% of the remaining NEE data, under the
190 assumption the NEE fluxes were likely affected by drilling activities. East winds were evenly
191 distributed over day (145 ° mean wind direction) and night (167 ° mean wind direction). Winds
192 originated from the east mostly during the winter (October to December) as regional-scale cold
193 fronts moved southward with winds blowing over peninsular Florida from the Atlantic Ocean
194 towards the Gulf of Mexico. Nevertheless, over ten-thousand NEE fluxes remained for trend

195 identification and gap-filling after the contamination filter at the Pine Upland site. Seasonal
196 trends were apparent and diurnal NEE variations were resolvable into surrogates for respiration
197 and photosynthesis, as described below.

198 Missing 30-minute fluxes (NEE, LE, H) were gap-filled using a look-up table approach
199 (Table 3) documented in Reichstein (2005). The look-up table replaces missing fluxes with
200 available fluxes collected during similar meteorological conditions (net radiation within 50 W m^{-2} ,
201 air temperature within 2.5°C and vapor pressure deficit within 5.0 Pa). Gap-filled fluxes are
202 grouped into “Filling Quality A, B, and C”. To briefly summarize, “Filling Quality A” gap-fills
203 based on the availability of various combinations of NEE, net radiation, air temperature and
204 vapor pressure deficit data that meet similarity requirements within a 1-hour to 14-day gap-
205 centered window. “Filling Quality B” gap-fills based on the availability of NEE, net radiation,
206 air temperature and vapor pressure deficit data that meet similarity requirements within a 1 to
207 140-day gap-centered window. “Filling Quality C” gap-fills based on averages of available NEE
208 data surrounding the gap. Reichstein (2005) contains further details regarding this gap-filling
209 algorithm.

210 Positive NEE during the night was assumed to represent ecosystem respiration (RE). RE
211 was weakly correlated with quantities such as air temperature ($R^2 = 0.01$ and 0.03 for linear and
212 exponential regression at Cypress Swamp, for example); thus, a statistical model was used for
213 predicting RE during the day. Daytime RE predictions were needed for gross ecosystem
214 exchange (GEE) estimates. The statistical model randomly estimated values for day-time RE
215 within one standard deviation of the mean RE over a day. For example, if 20 RE (+NEE) values
216 were available within a 24-hour period, the mean and standard deviation of RE was computed
217 using 20 available values. Subsequently, 28 daytime RE values were randomly predicted from a

218 range that was one standard deviation from the mean. Assuming day-time and night-time
219 respiration statistics are equal could be a source of error in our results. Identification of an
220 alternative for the RE statistical model was precluded by weak correlations between respiration
221 and ancillary variables such as air temperature.

222 Methane emissions (F_{CH_4}) at the Dwarf Cypress site were most problematic in terms of
223 missing 30-minute data. About 80% of the F_{CH_4} time series was missing, mostly due to poor
224 signal strength of the methane analyzer (signal strength filter <10). Furthermore, spikes in
225 methane fluxes were removed when the signal strength indicator (RSSI) changed by +/-10
226 between half-hourly time periods. Missing F_{CH_4} fluxes were distributed evenly over day and
227 night. Sub-daily gap-filling with the Reichstein (2005) lookup table and empirical regression
228 models was confounded by weak correlations with explanatory data, the greatest being $R^2 = 0.11$
229 with barometric pressure. Correlations were similarly weak when isolating methane emissions
230 between 10AM and 2PM; specifically, the greatest correlation ($R^2 = 0.12$) occurred with vapor
231 pressure deficit. Given weak sub-daily correlations, over six-thousand molar methane fluxes
232 were averaged by day and up-scaled to 357 molar fluxes of F_{CH_4} at daily resolution.

233 Seasonally, missing daily F_{CH_4} molar fluxes were more prevalent from 12/2012 to
234 5/2013; 10/2013 to 1/2014; 4/2014 to 5/2014; and 11/2014. Due to the seasonality of missing
235 data, a molar flux model was constructed (daily resolution) as a power function of continuous
236 variables that explained seasonality in methane emission, specifically, air temperature and
237 flooding at the Dwarf Cypress site. The methane model was expressed as:

238
$$F_{CH_4} = R e^{(BT_a(1+e^{a+b(stage)}))} \quad (2)$$

239 where T_a and $stage$ were mean daily air temperature (Celsius) and water distance above (+) or
240 below (-) land surface (meters), respectively. Least-squares regression defined values of

241 $R=0.008628$, $B=0.04$, $a=-3.8$, and $b=2.7$ that minimized sum-of-squared differences between
242 observed and computed F_{CH_4} molar fluxes (Figure 3). The F_{CH_4} model explained about 40
243 percent of the variability in mean daily F_{CH_4} fluxes.

244 Daily $-NEE$, RE , and F_{CH_4} were converted from molar to mass units. Gross daily mass
245 transfer of C from the atmosphere to the ecosystem (GEE, $g\text{ C m}^{-2}\text{ d}^{-1}$) was calculated as the sum
246 of NEE and RE during the day. Daily GEE, $-NEE$, RE and F_{CH_4} were summed to generate
247 monthly and annual C exchange totals. An upper bound for uncertainty in these totals was
248 approximated using a root mean square error propagating method (Topping, 1972). To
249 summarize, possible sources of error included random uncertainty (Finkelstein and Sims, 2001)
250 and gap-filling error. Gap-filling error was approximated using the standard error for $\pm NEE$ gap-
251 filling by Reichstein (2005). Standard errors were computed by creating artificial gaps (1, 5, 10
252 and 20% removal) in observed NEE and predicting fluxes during the artificial gaps with the
253 look-up table. The maximum standard error of the artificial gap scenarios was used to
254 approximate an upper bound for uncertainty, as follows:

255
$$U_{-NEE,RE} = \sqrt{\sum_{t=0}^{month} (U_r^2 + SE_{max}^2)} \quad (3)$$

256 where $U_{-NEE,RE}$ were monthly uncertainties in $-NEE$ or RE in $g\text{ C m}^{-2}$ per month, U_r was
257 random uncertainty (Finkelstein and Sims, 2001) in $g\text{ C m}^{-2}\text{ sec}^{-1}$, and SE_{max} was the maximum
258 standard error of the artificial gap scenarios (20% removal scenario - equal to 2.2, 1.1, and 2.0 g
259 $\text{C m}^{-2}\text{ sec}^{-1}$ for Cypress Swamp, Dwarf Cypress and Pine Upland, respectively). Uncertainty in
260 monthly GEE was the sum of uncertainty for $-NEE$ and RE . Uncertainty in F_{CH_4} was estimated
261 with Equation 3 using random uncertainty estimates (Finkelstein and Sims, 2001) for the
262 methane fluxes and the standard error (equal to $0.017\text{ g C m}^{-2}\text{ d}^{-1}$) of the methane flux model
263 (equation 2).

264 **3 Results and Discussion**

265 **3.1 Seasonality in Rainfall, Temperature, Water Levels and Energy Fluxes**

266 The subtropics of south Florida are characterized by distinct wet and dry seasons driven
267 by changes in solar insolation, air temperature, humidity, and rainfall. Rainfall and
268 photosynthesis are greatest in the hot and humid spring and summer months from about May to
269 October. The end of October generally marks the end of the wet season (and hurricane season).
270 Wetland water levels and surface energy fluxes are tightly coupled to seasonality in heat and
271 humidity. Cold fronts are especially remarkable within surface energy budgets, as dry cold air
272 passes over relatively warm soil and surface water, creating large variations in both stored-heat
273 energy and turbulent fluxes of heat and water vapor (Shoemaker et al., 2011).

274 During this study, air temperatures at all three sites (Figure 4 A-C) were seasonally
275 lowest (ranging from 15 to 25 °C) during December through March, and as low as 12 C for
276 several days during the passage of cold fronts in the winter. Cold fronts typically lasted 5 days
277 or less. During April and May, air temperatures rose above 25 C and were less variable as hot
278 and humid air masses dominated the subtropical region. By late May, air temperatures were
279 consistently 25 to 30 C and remained within this range until the onset of the dry season in mid-
280 to-late October. Water and soil temperatures (measured 0.15 m below land surface) were nearly
281 identical (absolute differences < 1 C) but were 1 to 5 C higher than air temperature during the
282 passage of cold fronts (Figure 4). Land surface served as a heat reservoir during cold fronts, and
283 water and soil temperatures seldom fell below 15 C. Cold fronts also increase vapor pressure
284 deficits due to cold, dry air moving rapidly over relatively wet and warm landscape.

285 Seasonality was observed in water levels at each site (Figure 4A, B and C) in response to
286 rainfall duration and intensity. Water levels were lower in the winter and early spring due to
287 reduced rainfall at the end of the dry season (i.e., November to May). Water levels rose in

288 response to rainfall at the end of April 2013 and May 2014, reaching ~1 m above land surface
289 during July through October at the Dwarf Cypress site. In contrast, water levels declined as
290 much as 1.0 m below land surface during the spring dry season from March to May 2014 (Figure
291 4A, B and C) creating an opportunity for enhanced soil respiration. Water levels remained
292 below land surface until rainfall in June 2014 eventually flooded each site.

293 Surface energy fluxes reflected the seasonality in air temperature and rainfall (Figure 4A,
294 B, C). Mean daily net radiation ranged from about 50 to over 200 W m⁻² and was greatest in the
295 summer months of June, July and August 2013 and 2014. Net radiation was least from
296 November to February when incoming solar radiation was seasonally smallest. Net radiation
297 was the primary driver of available energy and latent heat flux (Figure 4A, B, C), the energy
298 equivalent of evapotranspiration (ET). Mean daily latent heat fluxes ranged from about 0 to over
299 150 W m⁻² and were greatest in the summer months of June, July and August 2013 and 2014 at
300 the Cypress Swamp site. Latent heat fluxes were lowest from November to February when
301 incoming solar radiation was seasonally lowest, and less water was available for evaporation.
302 During these cooler and drier periods, transpiration also was limited by lower physiological
303 activity of trees, especially of the deciduous cypress trees (Figure 2B) during fall-winter leaf
304 drop (Figure 4B). Surface inundation combined with more incoming solar radiation resulted in
305 more energy partitioned as latent versus sensible heat during May to November. Also, cypress
306 leaves were notably greener during this period suggesting increased physiological activity and
307 seasonally higher transpiration rates.

308 **3.2 Carbon Exchange between the Atmosphere and Forested Wetlands**

309 All three sites were generally sinks of atmospheric carbon dioxide (CO₂) on daily,
310 monthly (Figure 5A, B, C) and annual time scales (Table 4). The sink strength of CO₂ at each
311 site, as evidenced by –NEE, was reduced during the fall and winter of 2012, 2013 and 2014

312 (Table 4, Figure 5). Seasonality in daily –NEE was least at Dwarf Cypress with –NEE ranging
313 from -1.0 to $-2 \text{ g C m}^{-2} \text{ d}^{-1}$ in the winter and summer, respectively. Seasonality in –NEE was
314 more extreme Cypress Swamp and Pine Upland with rates ranging from -1 to $-5 \text{ g C m}^{-2} \text{ d}^{-1}$ in
315 the winter and summer, respectively. Lack of forested vegetation at Dwarf Cypress likely
316 explains the dampened seasonality in C fluxes. Furthermore, pine trees grow and maintain
317 leaves all year (evergreen trees), which likely explains dampened seasonality in –NEE at Pine
318 Upland relative to Cypress Swamp.

319 The Moderate-resolution Imaging Spectroradiometer (MODIS) enhanced vegetation
320 index (EVI) served as a useful qualitative surrogate for seasonal terrestrial photosynthetic
321 activity and canopy structural variations (Figure 5), as reported for some other studies (Huete et
322 al. 2002). EVI over tall mangrove forest, for example, varied seasonally between 0.35 and 0.55,
323 and decreased to ~ 0.2 following defoliation after hurricane Wilma (Barr et al., 2013). Likewise,
324 EVI over evergreen forest (Xiao et al. 2004a) varied seasonally between 0.25 during the winter
325 and 0.5 during the summer growing season. EVI data were obtained from the MOD13A1
326 product of MODIS (EOS; <http://modis.gsfc.nasa.gov/>). Sixteen-day composite EVI values for
327 the pixel corresponding to each station, and the 8 adjacent pixels were extracted for comparison
328 with monthly C fluxes (Figure 5). This 9-pixel domain approximately corresponds with the
329 measurement footprint of each flux station.

330 Seasonal patterns in –NEE and GEE were consistent with changes in EVI (Figure 5A, B,
331 C), most notably at the Cypress Swamp site. Increases in EVI from 0.25 to 0.35 corresponded
332 with growth of cypress leaves on relatively tall (18 to 21 m) and densely-spaced cypress trees
333 (Figure 2) beginning in about March to April. Cypress leaves discontinued growing in August to
334 September and turned brown in October, eventually falling into the sawgrass and hardwood

335 understory. This lack of photosynthetic activity corresponded with changes in EVI from 0.4 in
336 the summer to 0.2 in the winter (Figure 5B) of 2013 and 2014 at the Cypress Swamp flux station.

337 Gross atmosphere-ecosystem C exchange (GEE) provides a first approximation of gross
338 ecosystem productivity (GEP), or accumulation of C in the plant canopy. Growth and
339 senescence of cypress leaves was most evident in monthly GEE (Figure 5, Table 4) at the
340 Cypress Swamp site, where rates increased from about 100 g C m^{-2} in February 2013 to over 200
341 g C m^{-2} in April 2013 (a 116 % increase). Likewise, GEE increased from about 100 g C m^{-2} in
342 February 2014 to about 300 g C m^{-2} in June 2014 (a 200 % increase). At the Dwarf Cypress site,
343 seasonal changes in GEE were more moderate; the February to April 2013 increase was from
344 about 60 g C m^{-2} to 100 g C m^{-2} (a 66 % increase). Foliage change at the Cypress Swamp site
345 likely contributed to a larger fraction of the site's change in photosynthetic CO_2 uptake compared
346 to that of the Dwarf Cypress site, which consists of a sparse cypress canopy (Figure 2) during the
347 height of the growing season (i.e., April to September).

348 A key water and ecosystem management issue in south Florida, and globally, is the
349 preservation of organic soils within wetlands (Hohner and Dreschel, 2015) to (1) support
350 ecosystem services, and (2) maintain or grow topography. Growing topography via C
351 accumulation in these coastal forested wetlands could partly offset sea-level rise. Inundation
352 suppressed respiration most remarkably at Cypress Swamp and Pine Upland (Figure 5A, B). RE
353 doubled from about 60 to 120 g C m^{-2} from February to May 2014 when water levels were below
354 land surface at Cypress Swamp (Figure 5B). Enhanced RE also was observed from March 2014
355 to July 2014 at Pine Upland (Figure 5A) when water levels were below land surface. Enhanced
356 RE was likely due to heterotrophic soil respiration supplementing autotrophic respiration when
357 water levels were below land surface for extended periods of time. These results suggest hydro-

358 period could be managed for maintenance of organic soils and peat accretion in these subtropical
359 cypress and pine forested wetlands.

360 **3.3 Links between C and Water Cycles**

361 Relationships between net ecosystem C exchange (-NEE) and latent heat flux (LE) reflect
362 an important link between water and C cycles (Figure 6); that is, photosynthesis that releases
363 water (transpiration) while storing C. R^2 between -NEE and LE provides an indication of the
364 relative magnitudes of transpiration and evaporation at each site. Stronger correlations between
365 NEE and LE indicate increased transpiration relative to evaporation, as water is transpired during
366 photosynthesis while the plant fixes C. In contrast, weaker correlations indicate a site with more
367 open water evaporation where the source for ET is less related to photosynthesis and more
368 related to evaporation from a water surface. Correlations between -NEE and LE were 0.35, 0.36
369 and 0.19 (Figure 6) at the Cypress Swamp, Pine Upland and Dwarf Cypress sites, respectively.
370 These correlations indicate transpiration is a larger portion of evapotranspiration at the forested
371 wetlands with larger and more densely spaced cypress and pine trees. Closed or partially closed
372 forested canopies reduced penetration of solar radiation to water surfaces, creating lowered lapse
373 rates between the water surface and canopy crown (Barr et al., 2012), and added resistance to
374 evaporation. Collectively, these results indicate a redistribution of plant communities toward
375 more open-water ecosystems (such as sparse sawgrass) could result in less C uptake and greater
376 evaporative losses. Prior studies of C accumulation further support this generalization; for
377 example, NEE rates were greater over mangrove systems (Barr et al., 2010; Barr et al., 2012)
378 than over sawgrass wetlands (Schedlbauer et al., 2010). Furthermore, prior ET studies (German,
379 2000) indicate ET losses are greater over wetlands with sparse sawgrass and open-water
380 conditions.

381 Coupling between water and C cycles was examined via water-use efficiencies (Table 5)
382 computed as the ratio of annual NEE to ET. As such, WUE are the net mass or moles of C
383 transferred to the ecosystem per mm or mole of water vapor. Computing WUE with NEE
384 accounts for the loss of C through Re. The Cypress Swamp and Pine Upland sites were most
385 efficient at using water to store C, with WUE equal to about 1.0 g C per mm ET (1.0 to 1.4
386 moles CO₂ per mole of ET). About 0.5 g C uptake occurs per mm of ET (0.7 moles CO₂ per
387 mole of ET) at the Dwarf Cypress site. Apparently, wetlands with more open-water surface
388 (Figure 2) are less efficient than forested wetlands at converting water use into net and gross C
389 uptake. This conclusion is likely to be true both regionally and perhaps globally, and thus, may
390 have implications for the global C cycle.

391 **3.3 Methane Emission**

392 Methane is produced by anaerobic bacteria decomposing organic matter in the soil or
393 surface water. Methane can be oxidized during transport from the soil or surface water into the
394 atmosphere. Transport to the atmosphere may occur through (1) roots and stems of vascular
395 plants (Wang and Han, 2005; Morrissey et al., 1993; Kim and Verma, 1998), (2) ebullition as gas
396 bubbles from anaerobic soils (Comas and Wright, 2012), and (3) diffusion through the soil and
397 surface water (Van Huissteden et al., 2006, Christensen et al., 2003a,b). Methane emission is
398 enhanced as anaerobic bacteria become more active at higher temperatures (Simpson et al.,
399 1995).

400 At the Dwarf Cypress site, methane emission increased with increasing air temperature
401 and water level in the summer months from June to September 2013 (Figure 5C). In contrast,
402 methane emission was suppressed from April to June 2014 due to dry conditions and perhaps the
403 memory of dry conditions from July to September 2014. Anaerobic bacteria may take some time
404 to reestablish following dry conditions. This reestablishment or “memory” of dry conditions

405 would reduce methane emission despite warm conditions and flooding from July to September
406 2014.

407 Methane emission peaked at different times in the summer of 2013 compared to GEE at
408 the Dwarf Cypress site (Figure 5C). GEE peaked with photosynthesis in July 2013 whereas
409 methane emission peaked in August 2013. This time lag indicates that processes governing C
410 exchange and methane emissions are quite different, with GEE controlled by photosynthesis of
411 cypress leaves and sawgrass which grow vigorously from March to April and discontinue growth
412 in August to September. In contrast, methane emission is driven by anaerobic decomposition of
413 organic matter with subsequent oxidation through the soil and surface water. Organic
414 decomposition was enhanced in August 2013 by flooding and relatively warm air, soil and
415 surface-water.

416 Although methane emission is important in terms of global warming potential (GWP), it
417 appears to be immaterial in C budgets that alter or “grow” land surface topography. C released
418 from methane emission was relatively small (averaging about 10 g C per year) compared to NEE
419 (about -500 g C per m² year, Table 4). Thus, C cycling studies that address changes in peat
420 accumulation may not benefit from monitoring methane fluxes. However, about 14 g CH₄
421 emission per year is roughly equivalent to 350 g CO₂, assuming the GWP of CH₄ is 25 times
422 greater than CO₂ (over a 100-year period, [IPCC 2007](#)). We recognize GWP multipliers are
423 controversial due to assumptions such as instantaneous CH₄ and CO₂ release, and time-scale
424 dependence of the radiative forcing contributions (Mitsch et al., 2013). Careful use of GWP
425 multipliers for wetlands is suggested.

426 **3.4 Comparison of C Uptake with Prior Studies**

427 Comparison of our results with –NEE from selected prior studies (Schedlbauer et al.
428 2010; Jimenez et al. 2012; Barr et al. 2010; Botkin et al. 1970; Jones et al. 2014) reveals

429 substantial spatial and temporal heterogeneity in C uptake over geologic time and among
430 different ecosystems (Table 6). Subtropical forested wetlands exchange more C than temperate
431 forests (Botkin et al., 1970; Sjogersten et al. 2014). A study assessing C exchange on a geologic
432 time scale (Jones et al. 2014) also concluded that long-term rates of C uptake in the Everglades
433 are higher than in northern latitudes, and in some cases rival C uptake in tropical peat-lands, such
434 as Indonesia. Mangrove ecosystems may serve as an upper limit for subtropical C uptake, with
435 NEE of about -1170 g C per m² year (Barr et al. 2010).

436 Sparse sawgrass wetlands in the Everglades, such as Taylor and Shark River Sloughs, are
437 relatively minor atmospheric C sources or sinks, with -NEE ranging from -50 (Taylor Slough) to
438 +45 (Shark River Slough) g C per m² year (Table 5). Jones et al. (2014) also concluded that
439 sloughs sequester the least amount of C in their study of C accumulation over geologic time
440 scales. Given the C released from methane emissions (10 g C per m² year, Table 4), as measured
441 at Dwarf Cypress (Figure 5C), sparse sawgrass wetlands may generally be atmospheric C
442 sources at monthly and annual time scales, with questionable value as local, regional and global
443 C sinks.

444 **4 Conclusions**

445 Atmospheric/ecosystem carbon dioxide exchange, methane emission, latent and sensible
446 heat fluxes were estimated with eddy covariance methods for subtropical forested cypress and
447 pine wetlands for two years. Seasonality in solar insolation, air temperature, plant physiological
448 activity, rainfall and water levels created seasonality in C exchange rates and surface energy
449 fluxes. Links between water and C fluxes also were revealed such as photosynthetic water-use
450 efficiencies.

451 Each forested wetland was an atmospheric C sink on monthly and annual time scales.
452 NEE was greatest at Cypress Swamp (-900 to -1000 g C per m² year), moderate at Pine Upland
453 (-650 to -700 g C per m² year), and least at Dwarf Cypress (-400 to -450 g C per m² year). The
454 size (about 20 m) and number of cypress trees enhanced C uptake at Cypress Swamp and
455 seasonality in C uptake rates was enhanced by the growth of cypress leaves in early April and
456 decay of cypress leaves in late October, as confirmed by changes in the satellite-derived EVI.
457 Changes in EVI (from 0.25 in the dry season to 0.4 in the wet season) served as a useful
458 surrogate for monthly and seasonal changes in net and gross ecosystem C exchange.

459 Respiration was enhanced when water levels dropped below land surface within these
460 cypress and pine forested wetlands. Increases in respiration were likely due to heterotrophic soil
461 respiration supplementing autotrophic respiration. These results highlight the importance of
462 flooding and hydro-period management for maintaining organic soils and peat accretion within
463 subtropical forested wetlands, a key water and ecosystem management issue in south Florida and
464 globally.

465 Links between water and C cycles were examined via (1) water-use efficiencies (WUE)
466 expressed as the ratio of annual NEE to ET, and (2) correlations between -NEE and LE.
467 Computing WUE with NEE accounts for the loss of C through respiration. The Cypress Swamp
468 and Pine Upland sites were most efficient at using water to store C, with WUE equal to about 1.0
469 g C per mm ET. About 0.5 g C was stored in the ecosystem per mm of ET at the Dwarf Cypress
470 site. These results indicate that wetlands with more open-water surface are less efficient at using
471 water to store C than forested wetlands. This pattern is likely to be true both regionally and
472 perhaps globally, and thus, may have implications for the global C cycle.

473 Correlations between -NEE and LE reflected photosynthesis which released water as
474 transpiration while storing C. The strength of the -NEE and LE correlation provided an
475 indication of the relative magnitudes of transpiration and evaporation at each site. Transpiration
476 was a large proportion of evapotranspiration at the Cypress Swamp and Pine Upland sites, as
477 indicated by correlations of 0.34, 0.36 and 0.18 for the Cypress Swamp, Pine Upland and Dwarf
478 Cypress sites, respectively. These results indicate that a redistribution of plant communities
479 toward more open-water ecosystems could create less C uptake and greater evaporative losses.

480 Methane emission at Dwarf Cypress was considerable in terms of global warming
481 potential, but immaterial in C budgets that build and maintain land-surface topography.
482 Approximately 14 g CH₄ was released into the atmosphere, roughly equivalent to 350 g CO₂,
483 assuming the global warming potential of CH₄ is about 25 times greater than CO₂. Methane
484 emission, however, did not reverse carbon accumulation for topography at Dwarf Cypress, as the
485 C released from methane emission (about 10 g C per m² year) was relatively small compared to
486 NEE (-500 g C per m² year). These results indicate that while methane monitoring is needed
487 when assessing the global warming potential of wetlands; C cycling studies that address changes
488 in topography and peat accumulation may not benefit from monitoring methane fluxes.

489 **5 Acknowledgements**

490 This study was funded, in part, by the U.S. Geological Survey (USGS) Greater
491 Everglades Priority Ecosystems Science (GEEES). Nick Aumen is acknowledged for helpful
492 conversations about the Everglades during project meetings and fieldwork in BCNP. Michael J.
493 Duever provided detailed vegetation descriptions and guidance during site selection. Steve
494 Krupa and Cynthia Gefvert from the South Florida Water Management District funded tower
495 construction. USGS peer reviews by Lisamarie Windham-Myers, Dave Sumner and Kim Haag

496 improved the quality of the manuscript. Biogeoscience peer reviews by Ankur Desai and an
497 anonymous referee also greatly improved the manuscript. Any use of trade, firm, or product
498 names is for descriptive purposes only and does not imply endorsement by the U.S. Government.

499 The data used to create this manuscript is openly available to the public at:

500 http://sofia.usgs.gov/exchange/carbon_exchange/

501

502

503 **6 References**

504 Alberto, M.C.R., Carmelita R., R. Wassmann, R.J. Buresh, J.R. Quilty, T.Q. Correa, J.M.
505 Sandro, Centeno C.A.R.: Measuring methane flux from irrigated rice fields by eddy covariance
506 method using open-path gas analyzer, *Field Crops Research* 160 (2014) 12–21, 2014.

507 Baldocchi, D.D., Hicks, B.B., and Meyers, T.P.: Measuring biosphere-atmosphere exchanges of
508 biologically related gases with micrometeorological methods: *Ecology*, v. 69, no. 5, p. 1331-
509 1340, 1988.

510 Barr, J.G., V.C. Engel, J.D. Fuentes, J.C. Zieman, T.L. O'Halloran, T.J. Smith III, and G.H.
511 Anderson G.H.: Controls on mangrove forest-atmosphere carbon dioxide exchanges in western
512 Everglades National Park. *Journal of Geophysical Research* 115, G02020, <http://dx.doi.org/10.1029/2009JG001186>, 2010.

513

514 Barr, J.G., V. Engel, T.J. Smith, and Fuentes J.D.: Hurricane disturbance and recovery of energy
515 balance, CO₂ fluxes and canopy structure in a mangrove forest of the Florida Everglades.
516 *Agricultural and Forest Meteorology* 153:54–66, <http://dx.doi.org/10.1016/j.agrformet.2011.07.022>., 2012.

517

518 Barr, J.G., V. Engel, J.D. Fuentes, D.O. Fuller, Kwon H.: Modeling light-use efficiency in a
519 subtropical mangrove forest equipped with CO₂ eddy covariance. *Biogeosciences*, 10, 2145–
520 2158, doi:10.5194/bg-10-2145-2013, 2013.

521 Botkin DB, GM Woodwell and Tempel N.: Forest productivity estimated from carbon dioxide
522 uptake, *Ecology* Volume 51, No. 6, 1057 – 1060, 1970.

523 Bridgham, S. D., J. P. Megonigal, J. K. Keller, N. B. Bliss, and Trettin C.: The carbon balance of
524 North American wetlands. *Wetlands* 26:889–916, 2006.

525 Campbell, G.S., and Norman, J.M.: An introduction to environmental biophysics: New York,
526 Springer, 286 p., 1998.

527 Comas, X., and Wright W.: Heterogeneity of biogenic gas ebullition in subtropical peat soils is
528 revealed using time-lapse cameras, *Water Resour. Res.*, 48, W04601,
529 doi:10.1029/2011WR011654, 2012.

530 Chapin, F.S., G.M. Woodwell, J.T. Randerson, E.B. Rastetter, G.M. Lovett, D.D. Baldocchi,
531 D.A. Clark, M.E. Harmon, D.S. Schimel, Valentini R.: Reconciling carbon- cycle concepts,
532 terminology, and methods. *Ecosystems* 9:1,041–1,050, <http://dx.doi.org/10.1007/s10021-005-0105-7>, 2006.

533

534 Christensen, T.R., Panikov, N., Mastepanov, M., Joabsson, A., Stewart, A., Oquist,
535 M., Sommerkorn, M., Reynaud, S., Svensson, B.: Biotic controls on CO₂ and CH₄ exchange in
536 wetlands—a closed environment study. *Biogeochemistry* 64,337–354, 2003a.

537 Christensen, T.R., Ekberg, A., Strom, L., Mastepanov, M., Panikov, N., Mats, O., Svensson,
538 B.H., Nykanen, H., Martikainen, P.J., Oskarsson H.: Factors controlling large scale variations in
539 methane emissions from wetlands. *Geophys. Res. Lett.* 30,
540 <http://dx.doi.org/10.1029/2002L016848>, 2003b.

541 Comas, X., and Wright W.: Heterogeneity of biogenic gas ebullition in subtropical peat soils is
542 revealed using time-lapse cameras, *Water Resour. Res.*, 48, W04601,
543 doi:10.1029/2011WR011654, 2012.

544 Duever, M.J., Carlson, J.E., Meeder, J.F., Duever, L.C., Gunderson, L.H., Riopelle, L.A.,
545 Alexander, T.R., Myers, R.L., and Spangler, D.P.: *The Big Cypress National Preserve: New*
546 *York*, National Audubon Society, 455 p., 1986.

547 Duever, M.J.: Southwest Florida Predevelopment Vegetation Map, *Map Publication of the South*
548 *Florida Water Management District*, 1 p., 2002.

549 Dyer, A.J.: Measurements of evaporation and heat transfer in the lower atmosphere by an
550 automatic eddy covariance technique: *Quarterly Journal of the Royal Meteorological Society*, v.
551 87, p. 401-412, 1961.

552 Finkelstein, P. L., and Sims, P. F.: Sampling error in eddy correlation flux measurements.
553 *Journal of Geophysical Research*, 106: 3503-3509, 2001.

554 German, E.R.: Regional evaluation of evapotranspiration in the Everglades: *U.S. Geological*
555 *Survey Water Resources Investigations Report 00-4217*, 48 p., 2000.

556 Hohner, S.M., Dreschel T.W.: Everglades peats: using historical and recent data to estimate
557 predrainage and current volumes, masses and carbon contents, *Mires and Peat*, Volume 16
558 (2015), Article 01, 1–15, <http://www.mires-and-peat.net/>, ISSN 1819-754X, 2015.

559 Huissteden JV, R. van den Bos, Alvarez I.M.: Modelling the effect of water table management
560 on CO₂ and CH₄ fluxes from peat soils *Neth. J. Geosci.: Geol. En Mijnbouw*, 85, 2006. pp. 3–
561 18., 2006.

562 Huete, A., K. Didan, T. Miura, E.P. Rodriguez, X. Gao, and Ferreira L.G.: Overview of the
563 radiometric and biophysical performance of the MODIS vegetation indices: *Remote Sensing of*
564 *Environment*, v. 83, no. 1, p. 195-213, 2002.

565 Jimenez, K.L., G. Starr, C.L. Staudhammer, J.L. Schedlbauer, H.W. Loescher, S.L. Malone, and
566 Oberbauer S.F.: Carbon dioxide exchange rates from short- and long-hydroperiod Everglades
567 freshwater marsh. *Journal of Geophysical Research* 117, G04009, <http://dx.doi.org/10.1029/2012JG002117>, 2012.

569 Jones, M.C., C.E. Bernhardt, Willard D.A.: Late Holocene vegetation, climate and land-use
570 impacts on carbon dynamics in the Florida Everglades, *Quaternary Science Reviews* 90 (2014)
571 90-105, 2014.

572 Kim J., Verma S.B.: Diel variation in methane emission from a midlatitude prairie wetland:
573 significance of convective through flow in *Phragmites australis*. *J. Geophys. Res.* 103, 29–39,
574 1998.

575 Mitsch W.J., Bernal B, Nahlik A.M., et al.: Wetlands, carbon, and climate change. *Landscape*
576 *Ecology* 28:583–597. doi: 10.1007/s10980-012-9758-8, 2013.

577 McPherson, B.F.: Vegetation map of southern parts of subareas A and C, Big Cypress Swamp,
578 Florida: U.S. Geological Survey Hydrologic Atlas HA-492, 1973.

579 Morrissey, L.A., Zobel, D.B., Livingston, G.P.: Significance of stomatal control on methane
580 release from Carex-dominated wetlands. *Chemosphere* 26, 339–355, 1993.

581 Parker G.G., G.E. Ferguson, and Love S.K.: Water resources of southeastern Florida, with
582 special reference to the geology and ground water of the Miami area, U.S. Geol. Surv. Water
583 Supply Pap., 1255, 965 pp., 1955.

584 Priestley, C.H.B., and Taylor R.J.: On the assessment of surface heat flux and evaporation using
585 large scale parameters: *Monthly Weather Review*, no. 100, p. 81–92, 1972.

586 Reichstein, M., E. Falge, D. Baldocchi, D. Papale, M. Aubinet, P. Berbigier, and R. Valentini.:
587 On the separation of net ecosystem exchange into assimilation and ecosystem respiration: review
588 and improved algorithm. *Global Change Biology*, 11(9): 1424-1439, 2005.

589 Schedlbauer, J., S. Oberbauer, G. Starr, and Jimenez K.L.: Seasonal differences in the CO₂
590 exchange of a short-hydroperiod Florida Everglades marsh. *Agricultural and Forest Meteorology*
591 150:994–1,006, <http://dx.doi.org/> 10.1016/j.agrformet.2010.03.005, 2010.

592 Shoemaker, W.B., and Sumner D.M.: Alternate corrections for estimating actual wetland
593 evapotranspiration from potential evapotranspiration: *Wetlands*, v. 26, no. 2, p. 528–543, 2006.

594 Shoemaker, W.B., and Lopez, C.D., and Duever M.: Evapotranspiration over spatially extensive
595 plant communities in the Big Cypress National Preserve, southern Florida, 2007–2010: U.S.
596 Geological Survey Scientific Investigations Report 2011–5212, 46 p., 2011.

597 Shoemaker W. B., Anderson F., Barr J. G., Graham S. L., and Botkin D. B.: Carbon exchange
598 between the atmosphere and subtropical forested cypress and pine wetlands, U.S. Geological
599 Survey, Data Set for the Dwarf Cypress site, doi:10.5066/F7ZG6Q94, 2015d.

600 Shoemaker W. B., Anderson F., Barr J. G., Graham S. L., and Botkin D. B.: Carbon exchange
601 between the atmosphere and subtropical forested cypress and pine wetlands, U.S. Geological
602 Survey Data Set for the Cypress Swamp site, doi:10.5066/F73776RZ, 2015e.

603 Shoemaker W. B., Anderson F., Barr J. G., Graham S. L., and Botkin D. B.: Carbon exchange
604 between the atmosphere and subtropical forested cypress and pine wetlands, U.S. Geological
605 Survey Data Set for the Pine Upland site, doi:10.5066/F7707ZG9, 2015f.

Simpson I.J., G.W. Thurtell, G.E. Kidd, M. Lin, T.H. Demetriades-Shah, I.D. Flitcroft, E.T. Kanemasu, D. Nie, K.F. Bronson H.U.: Tunable diode laser measurements of methane fluxes from an irrigated rice paddy field in the Philippines *J. Geophys. Res.*, 100 (1995), pp. 7283–7290, 1995.

606 Sjögersten S., C.R. Black, S. Evers, J. Hoyos-Santillan, E.L. Wright, and Turner B.L.: Tropical
607 wetlands: a missing link in the global carbon cycle? American Geophysical Union doi:
608 10.1002/2014GB004844.

609 Tanner, B.D. and Greene J.P.: Measurement of sensible heat and water vapor fluxes using eddy
610 correlation methods: Final report prepared for U.S. Army Dugway Proving Grounds, Dugway,
611 Utah, 1989.

612 Tanner, C.B., and Thurtell G.W.: Anemoclinometer measurements of Reynolds stress and heat
613 transport in then atmospheric surface layer: University of Wisconsin Technical Report ECOM-
614 66- G22-F, 82 p., 1969.

615 Tanner, B.D., Swiatek, E., and Greene J.P.: Density fluctuations and use of the krypton
616 hygrometer in surface flux measurements: Management of irrigation and drainage systems:
617 Irrigation and Drainage Division, American Society of Civil Engineers, July 21-23, 1993, Park
618 City, Utah, p. 945-952, 1993.

619 Topping, J.: Errors of Observation and Their Treatment. 4th ed. London, U.K.: Chapman and
620 Hall, 1972.

621 Troxler, T.G., E. Gaiser, J. Barr, J.D. Fuentes, R. Jaffé, D.L. Childers, L. Collado-Vides, V.H.
622 Rivera-Monroy, E. Castañeda-Moya, W. Anderson, R. Chambers, M. Chen, C. Coronado-
623 Molina, S.E. Davis, V. Engel, C. Fitz, J. Fourqurean, T. Frankovich, J. Kominoski, C. Madden,
624 S.L. Malone, S.F. Oberbauer, P. Olivas, J. Richards, C. Saunders, J. Schedlbauer, L.J. Scinto, F.
625 Sklar, T. Smith, J.M. Smoak, G. Starr, R.R. Twilley, Whelan K.: Integrated carbon budget
626 models for the Everglades terrestrial-coastal-oceanic gradient: Current status and needs for inter-
627 site comparisons: Oceanography, 26(3), 98-107, 2013.

628 Twine, T.E., Kustas, W.P., Norman, J.M., Cook, D.R., Houser, P.R., Meyers, T.P., Prueger, J.H.,
629 Starks, P.J., Wesely M.L.: Correcting eddy-covariance flux underestimates over a grassland.
630 Agricultural and Forest Meteorology 103, 279–300, 2000.

631 Huissteden V., J., van den Bos, R., Alvarez I.M.: Modelling the effect of watertable management
632 on CO₂and CH₄fluxes from peat soils. Neth. J. Geosci.: Geol. En Mijnbouw 85, 3–18, 2006.

633 Wang, Z.P., Han X.G.: Diurnal variation in methane emissions in relationto plants and
634 environmental variables in the Inner Mongolia marshes. Atmos. Environ. 39, 6295–6305, 2005.

635 Webb, E.K., Pearman, G.I., Leuning R.: Correction of flux measurements for density effects due
636 to heat and water vapour transfer. Quarterly Journal of the Royal Meteorological Society 106,
637 85–100, 1980.

638 Whalen S.C.: Biogeochemistry of methane exchange between natural wet-lands and the
639 atmosphere. Environ. Eng. Sci. 22, 73–94, 2005.

640 Xiao, X., D. Hollinger, J.D. Aber, M. Goltz, E. Davidson, Q. Zhang, and B. Moore III.:
641 Modeling gross primary production of temperate deciduous broadleaf forest using satellite
642 images and climate data. Remote Sensing of Environment 91 (2004) 256 – 270, 2004a.

643

644 Table 1. Site locations, tower heights and summary of vegetation.

Site	Latitude	Longitude	Height of	Height of	Vegetation
			tower (m)	vegetation (m)	
Dwarf Cypress	25.7624	-80.8934	16.8	0.5 to 10	Small cypress and sawgrass
Cypress Swamp	25.8265	-81.1020	38.1	0.5 to 21	Tall cypress
Pine Upland	26.0004	-80.9260	38.1	0.5 to 21	Pine, sawgrass and cypress

645

646

647

648

649 Table 2. Instrumentation installed at the Dwarf Cypress, Cypress Swamp and Pine Upland flux
 650 stations.

		Distance above or below land surface, in meters			
Instrument	Model	Measurement	Dwarf Cypress	Pine Upland	Cypress Swamp
Sonic anemometer	CSAT ¹ , Gill Windmaster Pro ²	Wind velocity and direction	15.5	35.8	35.7
Gas analyzer	LI-7500A	Gas concentrations	15.5	35.8	35.7
Methane analyzer	LI-7700	Methane concentration	15.5	NA	NA
Pressure transducer	CS450	Water depth	-0.8	-0.5	-0.5
Air temperature	HMP-45C	Air temperature	15.5	35.8	35.8
Relative humidity	HMP-45C	Relative humidity	15.5	35.8	35.8
Net radiometer	NR-Lite	Net radiation	13.2	33.7	33.9
Soil heat flux	REB's	Soil heat flux	-0.2	-0.2	-0.2
Soil temperature	107L	Soil temperature	-0.2	-0.2	-0.2

651 ¹CSAT deployed at the Dwarf Cypress and Pine Upland sites.

652 ²Gill Windmaster Pro deployed at the Cypress Swamp site.

654 Table 3. Gap-filling results for fluxes based on the look-up table approach by Reichstein et al.
 655 (2005).

Cypress Swamp	H¹	LE²	NEE
Filling Quality A	8239	10591	11506
Filling Quality B	32	34	31
Filling Quality C	9	9	13
Total gap-filled	8280	10634	11550
Total fluxes	34848	34848	34848
Percent rejected	24	31	33
Dwarf Cypress	H	LE	NEE
Filling Quality A	6830	8365	9828
Filling Quality B	389	398	393
Filling Quality C	70	70	74
Total gap-filled	7289	8833	10295
Total fluxes	35328	35328	35328
Percent rejected	21	25	29
Pine Upland	H	LE	NEE
Filling Quality A	9001	9997	23554
Filling Quality B	138	139	174
Filling Quality C	243	242	393
Total gap-filled	9382	10378	24121
Total fluxes	35424	35424	35424
Percent rejected	26	29	68

656 ¹Sensible heat flux. ²Latent heat flux.

657

658

659

660

661

662

663 Table 4. Monthly and annual C and methane fluxes.

	Cypress Swamp			Dwarf Cypress				Pine Upland		
Month	-NEE ¹	Re ¹	GEE ¹	-NEE ¹	Re ¹	GEE ¹	CH ₄ ¹	-NEE ¹	Re ¹	GEE ¹
Dec-12	-19±4	31±2	49±6	-18±1	27±1	45±3	0.6±0.003	-52±3	45±6	96±10
Jan-13	-30±5	51±2	81±8	-25±1	35±3	59±5	0.6±0.004	-54±4	63±6	117±10
Feb-13	-31±4	57±2	87±6	-22±4	43±3	65±7	0.5±0.003	-40±4	60±11	100±15
Mar-13	-75±3	83±2	157±5	-27±2	39±2	66±5	0.5±0.002	-59±4	69±8	127±12
Apr-13	-98±5	117±3	215±8	-50±3	45±4	94±7	0.6±0.003	-62±5	82±14	143±20
May-13	-123±5	99±3	221±9	-61±3	45±3	106±6	0.6±0.006	-89±5	64±13	152±19
Jun-13	-131±5	68±3	199±8	-58±5	43±3	101±8	1.1±0.005	-88±6	56±20	143±26
Jul-13	-107±5	51±3	157±9	-59±3	43±1	102±4	1.5±0.006	-103±6	54±22	157±29
Aug-13	-96±6	53±4	149±10	-45±3	37±3	82±7	2.3±0.011	-82±4	41±15	122±19
Sep-13	-67±6	61±3	128±10	-32±4	36±4	68±8	2±0.004	-45±4	58±11	103±16
Oct-13	-51±4	55±2	106±7	-27±2	28±1	55±4	1.7±0.004	-29±3	44±9	73±13
Nov-13	-42±5	61±3	103±15	-24±2	32±3	55±6	0.8±0.004	-11±4	39±12	50±17
Annual total	-865±61	794±37	1658±106	-443±39	461±36	903±76	13±0.06	-708±58	681±153	1389±211
Dec-13	-29±4	53±2	82±7	-23±2	31±2	54±4	0.7±0.004	-12±4	34±10	45±14
Jan-14	-30±5	51±3	80±8	-19±2	32±3	51±5	0.5±0.002	-28±4	45±9	73±13
Feb-14	-29±5	55±3	84±9	-22±1	28±2	49±4	0.8±0.002	-64±4	42±9	105±13
Mar-14	-64±5	84±3	147±8	-34±2	40±2	73±5	0.6±0.002	-55±4	76±16	130±21
Apr-14	-119±5	127±3	245±9	-46±3	55±3	100±6	0.6±0.004	-73±4	88±12	160±17
May-14	-136±5	141±3	276±9	-39±3	58±3	97±6	0.6±0.004	-64±5	121±13	185±18
Jun-14	-125±1	101±0	226±2	-48±2	53±2	101±4	0.6±0.001	-64±1	134±5	198±6
Jul-14	-131±4	68±3	198±8	-45±2	41±2	86±4	0.6±0	-89±5	83±20	172±26
Aug-14	-125±5	67±3	191±9	-34±2	41±1	75±4	0.5±0.009	-75±5	52±17	126±23
Sep-14	-81±5	68±3	148±8	-32±4	39±4	71±8	0.4±0.006	-77±6	64±19	140±25
Oct-14	-62±5	67±3	129±8	-24±2	32±2	56±4	0.4±0.007	-51±3	48±4	98±8
Nov-14	-32±4	68±2	99±7	-16±3	26±3	41±6	0.6±0.001	-27±3	46±11	72±14
Annual total	-956±60	954±37	1909±97	-377±33	481±33	858±66	7±0.04	-673±54	837±150	1509±205

664 ¹Units are g C /m² month or g C /m² year for net ecosystem exchange (NEE), respiration (Re),

665 gross exchange (GEE) and methane production (CH4).

666

667 Table 5. ET, NEE and WUE at the flux stations.

Site	ET ¹	-NEE ²	WUE ³
Pine Upland	1050(yr1 ⁴) 1070 (yr2 ⁵)	-700(yr1 ⁴) -700 (yr2 ⁵)	0.7 / 1.0 (yr1 ⁴) 0.7 / 1.0 (yr2 ⁵)
Dwarf Cypress	970(yr1 ⁴) 900 (yr2 ⁵)	-450(yr1 ⁴) -400 (yr2 ⁵)	0.5 / 0.7 (yr1 ⁴) 0.4 / 0.7 (yr2 ⁵)
Cypress Swamp	1000(yr1 ⁴) 1100 (yr2 ⁵)	-900(yr1 ⁴) -1000 (yr2 ⁵)	0.9 / 1.4 (yr1 ⁴) 0.9 / 1.4 (yr2 ⁵)

668 ¹Units are millimeters per year

669 ²Units are g C per year

670 ³Units are g C per millimeter ET or (/) moles CO₂ per mole ET

671 ⁴ yr1 from 12/1/2012 to 11/30/2013.

672 ⁵ yr2 from 12/1/2013 to 11/30/2014.

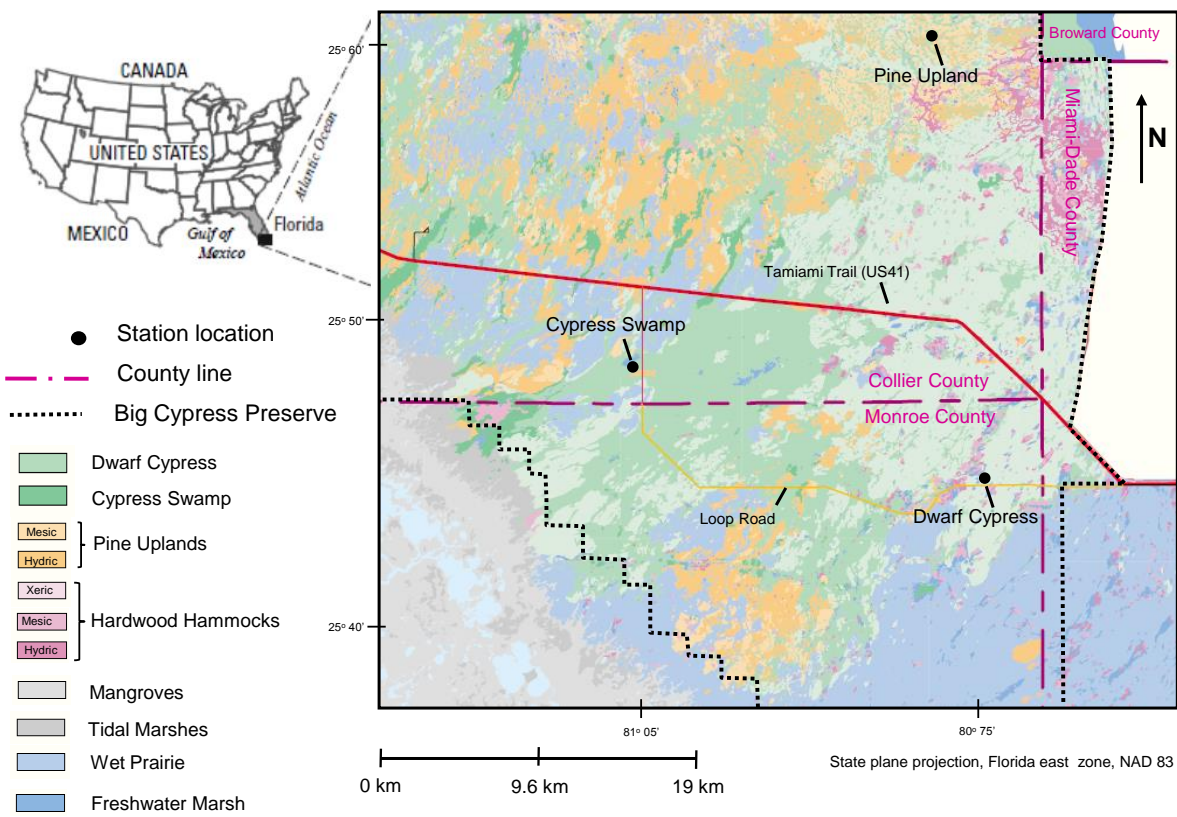
673

674 Table 6. Comparison of annual totals for NEE for different studies.

Ecosystem	NEE¹	Climate	Reference
Taylor Slough (short sawgrass)	-50	Subtropics	Schedlbauer (2010)
Shark River Slough (short sawgrass)	45	Subtropics	Jimenez (2012)
Mangrove	-1170	Subtropics	Barr (2010)
Cypress Swamp	-900 to -1000	Subtropics	This study
Dwarf Cypress	-400 to -500	Subtropics	This study
Pine Upland	-750 to -800	Subtropics	This study
White Oak	-296	Temperate	Botkin (1070)
Scarlet Oak	-274	Temperate	Botkin (1070)
Pitch Pine	-124	Temperate	Botkin (1070)
Everglades	-100 to > -200	Subtropics	Jones et al. (2014)

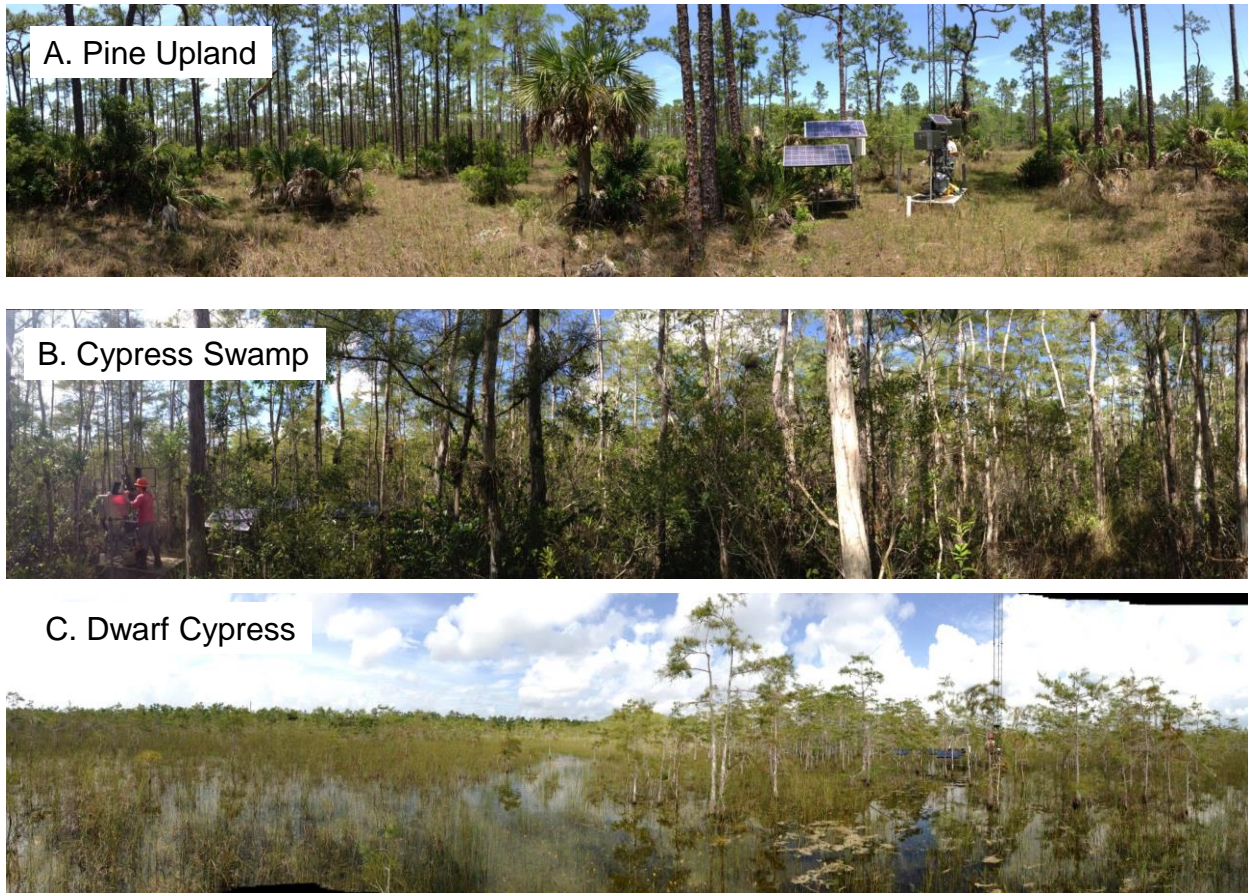
675 ¹Units are g C per m² year

676



679 Figure 1. Location of the study area and vegetation communities, modified from Duever (2002).

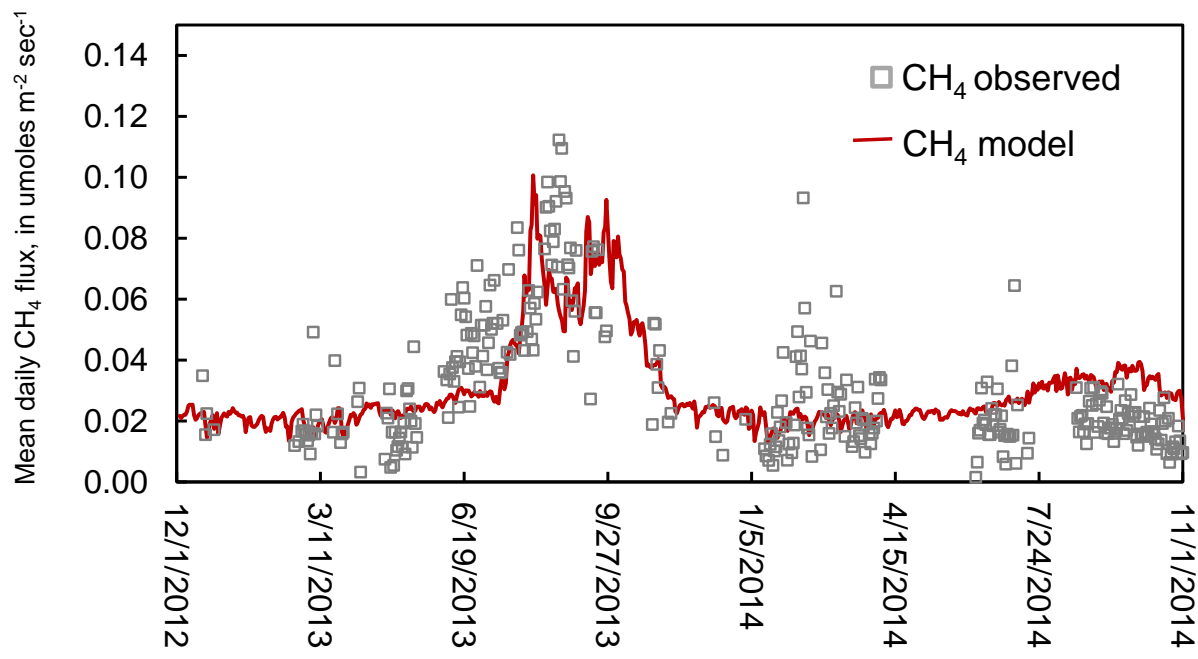
681



682

683 Figure 2. Panoramic photos of the (A) Pine Upland, (B) Cypress Swamp, and (C) Dwarf Cypress
684 plant communities.

685



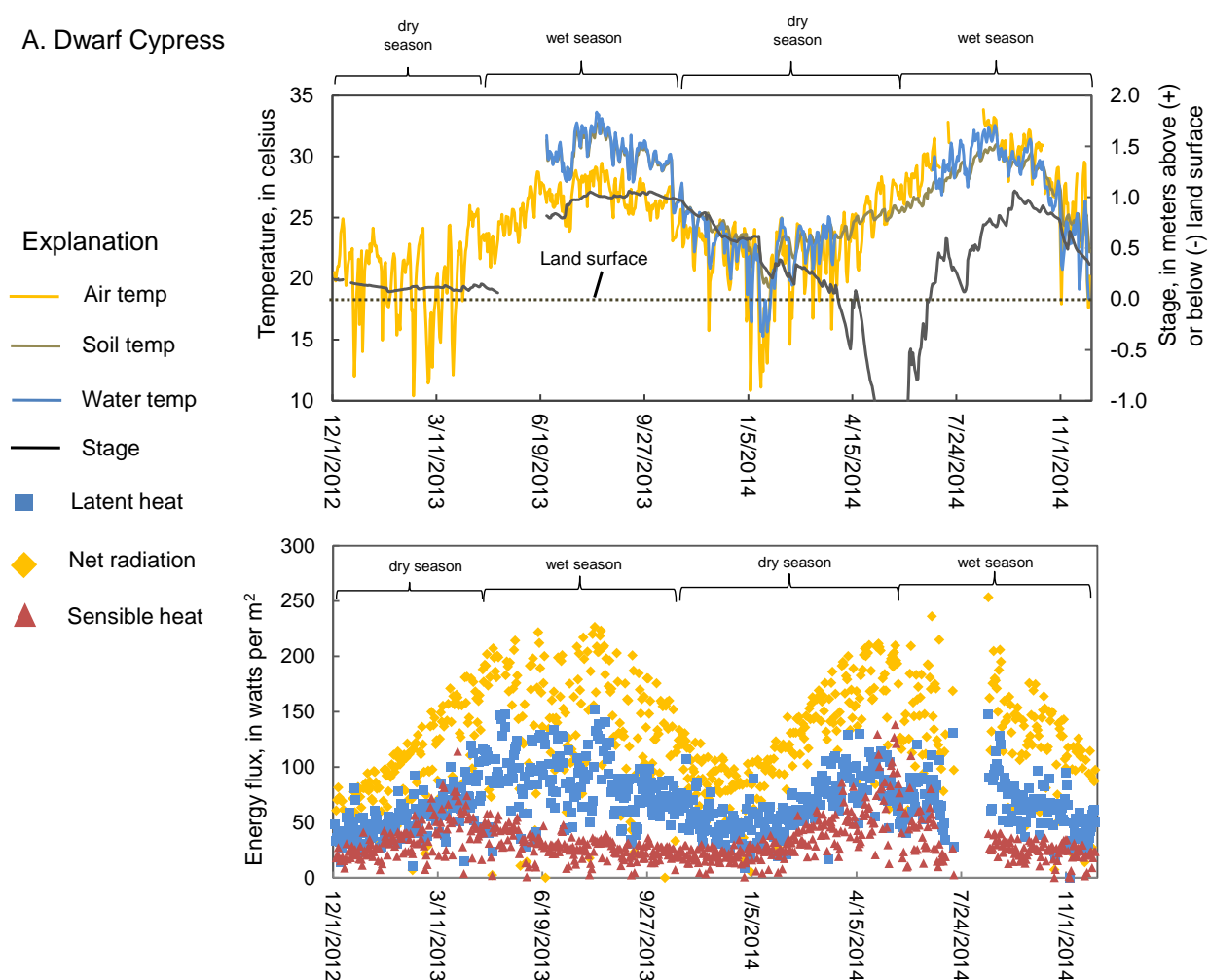
686
687

688 Figure 3. Observed and computed mean daily molar methane (CH_4) flux at the Dwarf Cypress
689 site.

690

691

A. Dwarf Cypress



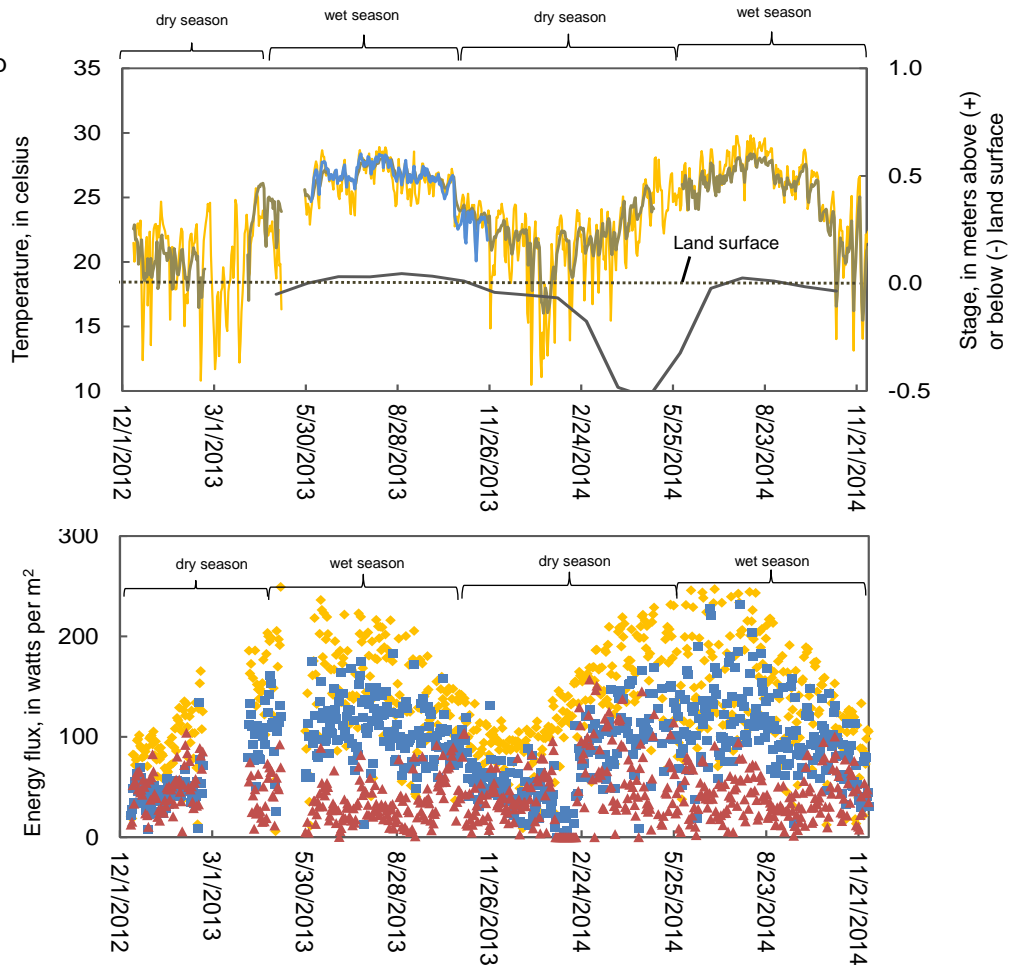
692

693

B. Cypress Swamp

Explanation

- Air temp
- Soil temp
- Water temp
- Stage
- Latent heat
- ◆ Net radiation
- ▲ Sensible heat



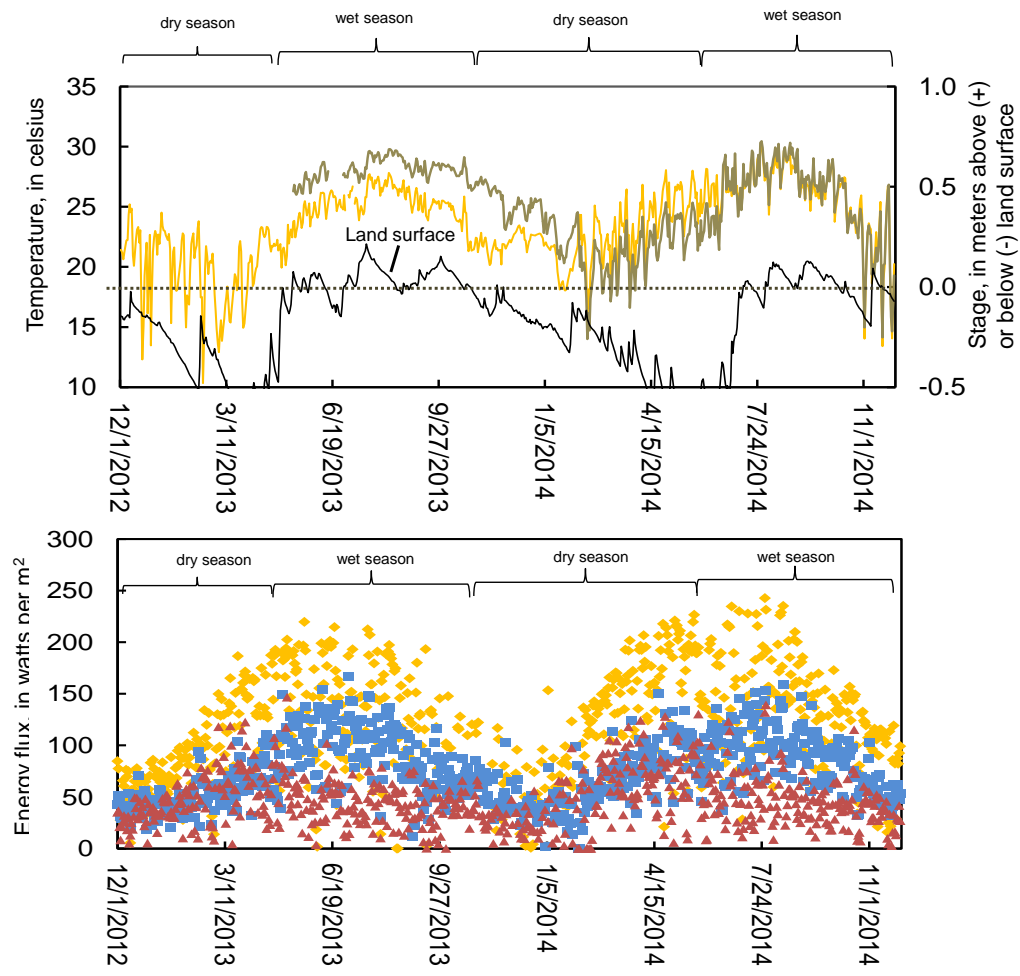
694

695

C. Pine Upland

Explanation

- Air temp
- Soil temp
- Water temp
- Stage
- Latent heat
- ◆ Net radiation
- ▲ Sensible heat



696

697

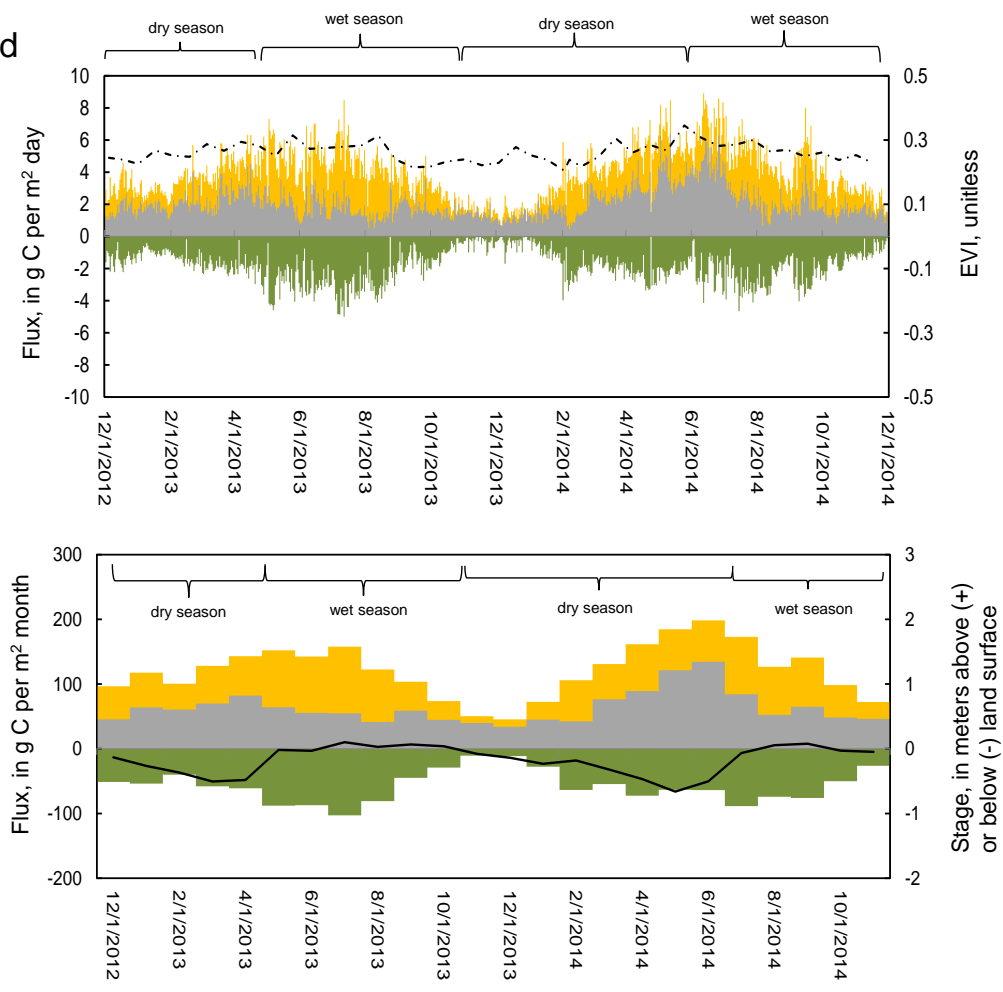
698 Figure 4A, B, C. Mean daily temperature and surface energy fluxes.

699

A. Pine Upland

Explanation

- GEE
- Re
- -NEE
- - - EVI
- Stage

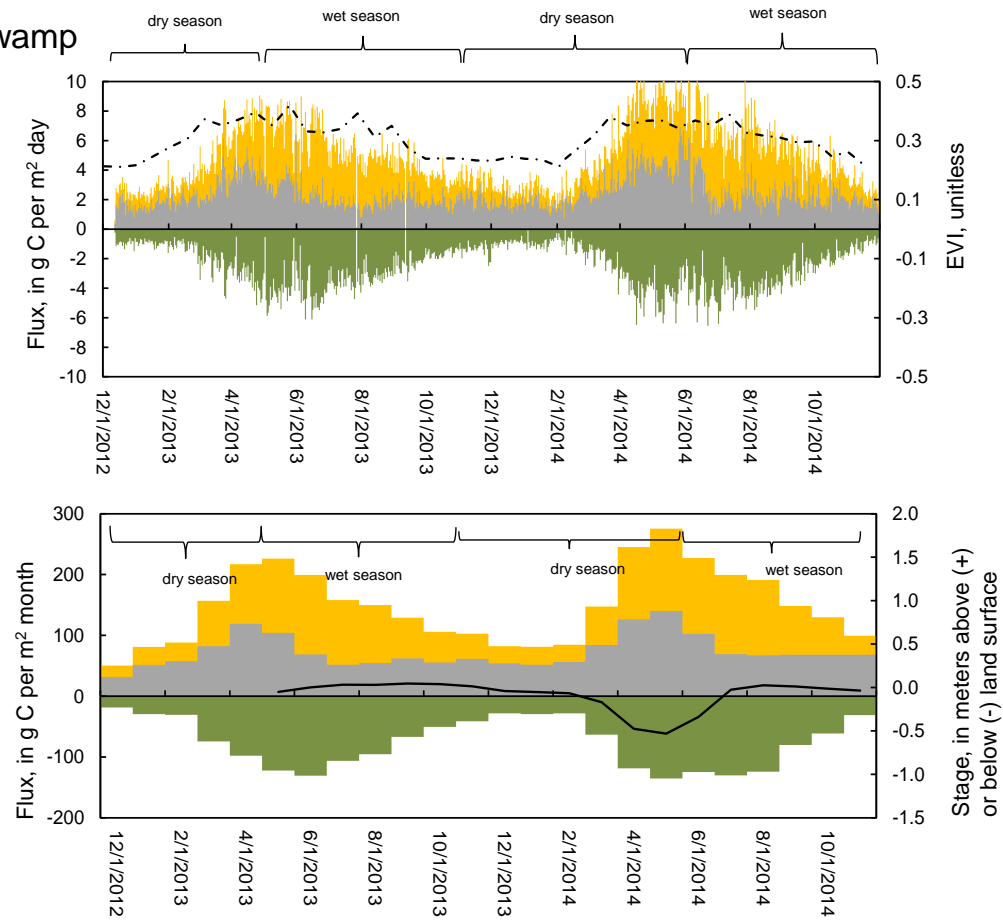


700
701

B. Cypress Swamp

Explanation

- GEE
- Re
- -NEE
- - - EVI
- Stage



702

703

704

705

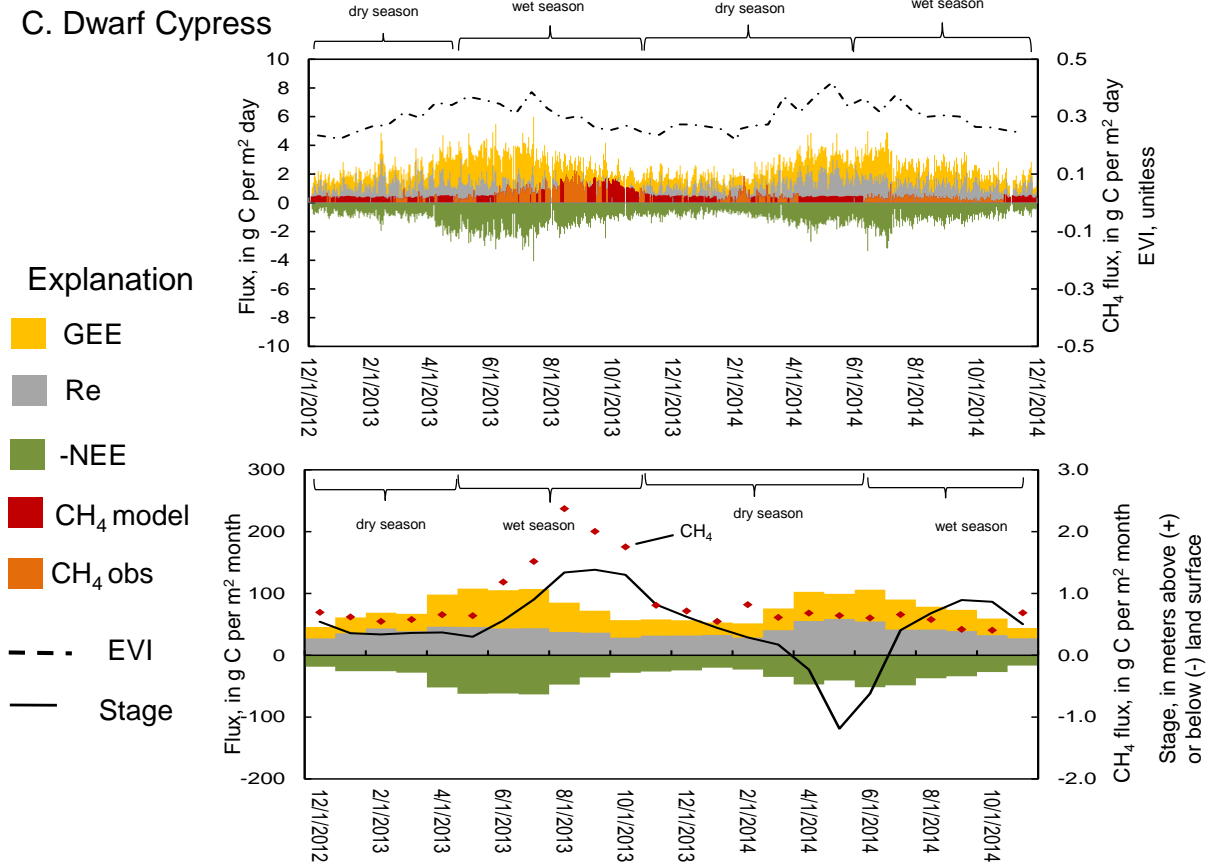
706

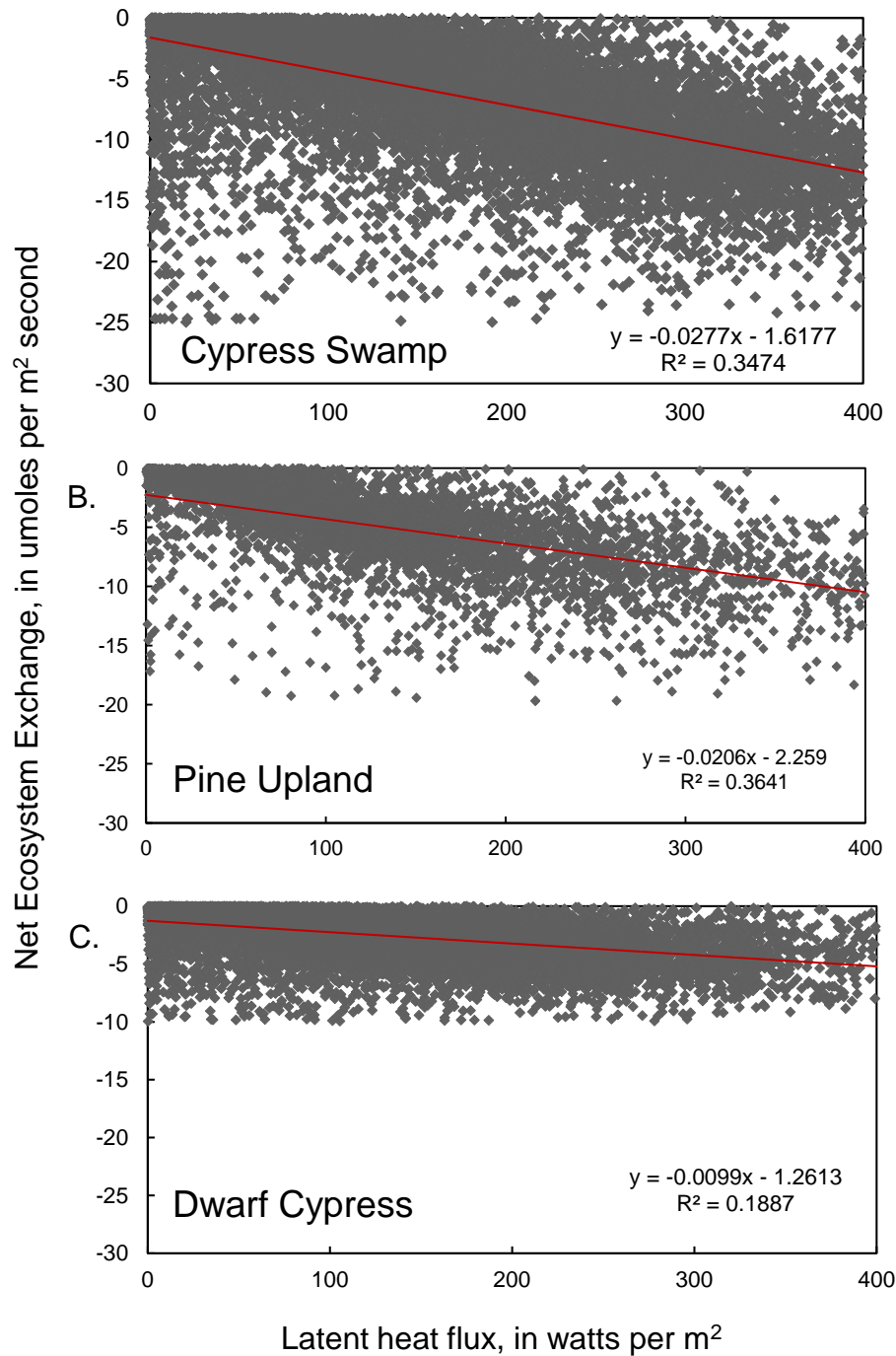
707

708

709

710
711
712 C. Dwarf Cypress





715

716 Figure 6. Relations between latent heat flux and net ecosystem exchange.